ACS APPLIED MATERIALS & INTERFACES

Research Article

www.acsami.org

Effect of the Thermal Conductivity on Resistive Switching in GeTe and $Ge_2Sb_2Te_5$ Nanowires

Sungjin Park,[†] Dambi Park,[†] Kwangsik Jeong,[†] Taeok Kim,[†] SeungJong Park,[†,⊥] Min Ahn,[†] Won Jun Yang,[†] Jeong Hwa Han,[†] Hong Sik Jeong,[‡] Seong Gi Jeon,[§] Jae Yong Song,[∥] and Mann-Ho Cho*[,†]

[†]Institute of Physics and Applied Physics, Yonsei University, Seoul, 120-749 Korea

[‡]School of Integrated Technology, Yonsei University, Incheon, 406-840 Korea

[§]Department of Materials Science and Engineering, Korea Advanced Institute of Science and Technology, Daejeon 305-701, Republic of Korea

[∥]Korea Research Institute of Standards and Science, Daejeon 305-340, Republic of Korea

Supporting Information

ABSTRACT: The thermal conduction characteristics of GeTe and $Ge_2Sb_2Te_5$(GST) nanowires were investigated using an optical method to determine the local temperature by Raman spectroscopy. Since the localization of surface charge in a single-crystalline nanostructure can enhance charge-phonon scattering, the thermal conductivity value (κ) of single crystalline GeTe and GST nanowires was decreased significantly to 1.44 Wm^{-1} K^{-1} for GeTe and 1.13 Wm^{-1} K^{-1} for GST, compared to reported values for polycrystalline structures. The SET-to-RESET state in single-crystalline GeTe and GST nanowires are characteristic of a memory device. Unlike previous reports using GeTe and GST nanowires, the SET-to-RESET characteristics showed a bipolar switching shape and no unipolar switching. In addition, after multiple cycles of operation, a significant change in morphology and composition was observed without any structural phase transition, indicating that atoms migrate toward the cathode or anode, depending on their electronegativities. This change caused by a field effect indicates that the structural phase transition does not occur in the case of GeTe and GST nanowires with a significantly lowered thermal conductivity and stable crystalline structure. Finally, the formation of voids and hillocks as the result of the electromigration critically degrades device reliability.

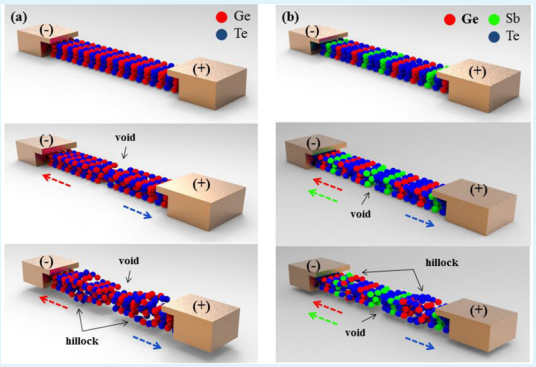

KEYWORDS: *$Ge_2Sb_2Te_5$, GeTe, phase-change memory, thermal conductivity, bipolar switching property*

Tellurides have been the predominant materials for thermoelectric, memory, and sensor applications in the past decade. In particularly, GeTe and $Ge_2Sb_2Te_5$(GST) are well-known tellurides of interest for many electrical applications. These are traditional phase change RAM (PRAM) materials that have attracted attention in the past due to excellent phase change performance[1−3] and potential for thermal[4] and chemical[5] sensors. In addition, interest in GeTe and GST has further increased because of its promising technological applications in thermoelectric and topological insulators.[6−8] Recently, to improve the physical and electrical property of GeTe and GST, many researchers have focused on investigating the synthesis of nanostructure. In nanosized electronics, because of scale down in the device, thermal properties play a critical role for device reliability, because a undesirable cell operation can occur due to the transport of heat to an adjacent cell. Moreover, in chalcogenide based electronics, the heat transport process can affect phase transition through nucleation and growth processes, resulting in a change in device performance. Therefore, in designing a nanosize chalcogenide device array, thermal properties are essential and need to be considered. However, most previous reports have focused on synthesis methods or the performance of electrical devices.[9−11] For these reasons, we investigated the thermal properties of the GeTe and GST nanowires and correlations between the effect of the thermal conductivity of GeTe and GST nanowires and electrical operation properties.

Generally, to measure the thermal conductivity of a nanowire, the 3ω method is used.[12−14] However, the fabrication of a floating device structure for use in such measurements is not easy. Since the device is destroyed during the measurement process when the 3ω method is used, many researchers have recently considered the use of a non-destructive measurement method, such as Raman spectrosco-

Received: June 26, 2015
Accepted: September 15, 2015
Published: September 15, 2015

DOI: 10.1021/acsami.5b05703
ACS Appl. Mater. Interfaces 2015, 7, 21819−21827

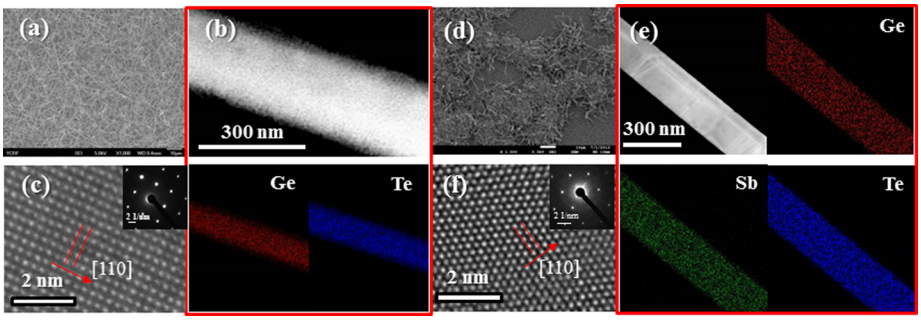

Figure 1. SEM (a) and HRTEM (c) image of GeTe nanowire synthesized by the VLS method. Inset of part c shows the corresponding SAED pattern of the GeTe nanowire with axis along [110]. (b) STEM and elemental mapping image of the GeTe nanowire clearly shows that Ge and Te elements are uniformly distributed in the nanowire. SEM (d) and HRTEM (f) image of GST nanowire synthesized by a VLS method. Inset of (f) shows the corresponding SAED pattern of the GST nanowire with the axis along [110]. (e) STEM and elemental mapping image of the GST nanowire shows that Ge, Sb, and Te elements are uniformly distributed over the whole nanowire. The index of electron diffraction patterns is presented in Figure S2.

py.[15−19] In this method, sample preparation is easy and repeated measurements are possible without any destruction of the sample because a direct thermal heating process is not involved in Raman spectroscopy. Since the reported values for the thermal conductivity in nanostructure such as IV, III−V group nanowires, MoS_2 and graphene have been confirmed to be reliable compared with values obtained by simulation or the 3ω method, it is considered to be a useful method for evaluating thermal conductivity.[21−23]

In this study, we successfully synthesized GeTe and GST nanowires with a single-crystalline structure. To obtain the thermal conductivity value using this optical method, information on the shape of nanostructure, laser power absorbed in nanostructure, and the impact of temperature variation with Raman frequency was investigated. Importantly, a detailed temperature-dependent Raman study of GeTe and GST nanowires was performed. To isolate substrate effects, the Raman frequency was measured for the case of suspended GeTe and GST nanowires. Using this noncontact method, it was possible to monitor local temperature variations in nanowires caused by laser heating. This method permits the role of thermal conduction in a electrical device as well as carrier scattering with phonon in nanowires to be evaluated. To estimate the laser power absorbed in nanowire, a finite-difference time-domain (FDTD) method was used.[24] Using these results, the thermal conductivities of GeTe and GST nanowires were determined to be 1.44 W/mK for GeTe and 1.13 W/mK for GST. Because of surface effects in nanowires such as localized charge within the surface region, these values are lower than the values reported using GeTe and GST films. The low thermal conductivity critically affected structural destruction during the electrical operation under an electrical pulse. Therefore, the change in thermal conductivity value of GeTe and GST nanostructures appear to be very important aspects to be considered in the design of GeTe and GST based electronics, optics, and thermoelectronics for the fabrication of devices with reliable characteristics.

EXPERIMENTS

GeTe and GST nanowires were synthesized based on a vapor−liquid−solid (VLS) method with GeTe and GST powder, respectively. Si substrates with 3 nm-thick Au films were placed at the downstream side of a tube furnace. GeTe and GST powder were located in the upstream side of the furnace. The furnace temperature was ramped up to 600 °C to vaporize the GeTe and GST with Ar/H_2 as the carrier gas (50/10 sccm) at a pressure of 2.4 Torr. The growth temperatures of the GeTe and GST nanowires were maintained at 300 and 340 °C for a reaction time of 5 h, respectively. A morphological analysis, based on scanning electron microscopy (SEM) observations, performed by a JEOL 7001F field emission microscope at an accelerating voltage of 10 kV. Analytical and conventional transmission electron microscopy (TEM) studies were performed on Cu grids with dispersed nanowires using a high-resolution (0.1 nm) field emission JEOL JEM-2200FS microscope at an accelerating voltage of 200 kV, equipped with energy-dispersive X-ray spectroscopy (EDS). To investigate the thermal conductivity (κ) of GeTe and GST nanowires, temperature-dependent Raman spectra, and local heating properties were measured in a single nanowire suspended from two supporting electrodes using a Nanofinder30 micro-Raman spectrometer interfaced with an excitation laser with a wavelength of 633 nm and spot size of ~1 μm and linkam stage. To measure temperature-dependent Raman spectra, Raman spectra of the GeTe and GST nanowires were measured at specific temperatures using a heated linkam stage. All measurements were carried out with a laser power of 0.13 mW and a measurement time of 20 s. A model of the expected temperature profile on the suspended part of the nanowire can be simply described as follows.[20]

$$\Delta T(x) = -\frac{P_{abs}}{\kappa A}\left(\frac{x^2}{L} - \frac{L}{4}\right) = -B_1 x^2 + \Delta T_{max} \quad (1)$$

where P_{abs} is the absorbed Raman laser power in the nanowire, L is the length of the suspended part, A is the cross section area, and B_1 is the curvature. The origin of the coordinate system is set to the center of the suspended part. Using a maximum temperature difference, the ΔT_{max} thermal conductivity is defined as

$$K = \frac{P_{abs} L}{4\Delta T_{max} A} \quad (2)$$

where the P_{abs} was calculated by FDTD simulation. For the evaluation of P_{abs} using FDTD, the optical constant n (refractive index) and k (extinction coefficient) of GeTe and GST at 633 nm were needed. To find the n and k value for GeTe (rhombohedral structure) and GST (hexagonal structure), we used DFT calculations. Our DFT calculations were performed using the Vienna ab initio simulation package (VASP) with projector-augmented wave (PAW) pseudopotentials under a cutoff energy of 500 eV for the plane wave expansion of the wave functions. We also used the GGA (Generalized Gradient Approximation) with the PBEsol (Perdew−Burke−Ernzerhof exchange-correlation density functional) exchange correlation function. In order to have a k-spacing of less than 0.25, a k-point mesh of 9 × 9 × 9 was chosen to obtain well-converged results. The calculated n/k value of GeTe and GST was determined to be 4.91/4.8 and 3.9/1.9 respectively.

In the case of ΔT_{max}, it is defined using the value of Raman frequency shift with the change in temperature and temperature profile

DOI: 10.1021/acsami.5b05703
ACS Appl. Mater. Interfaces 2015, 7, 21819−21827

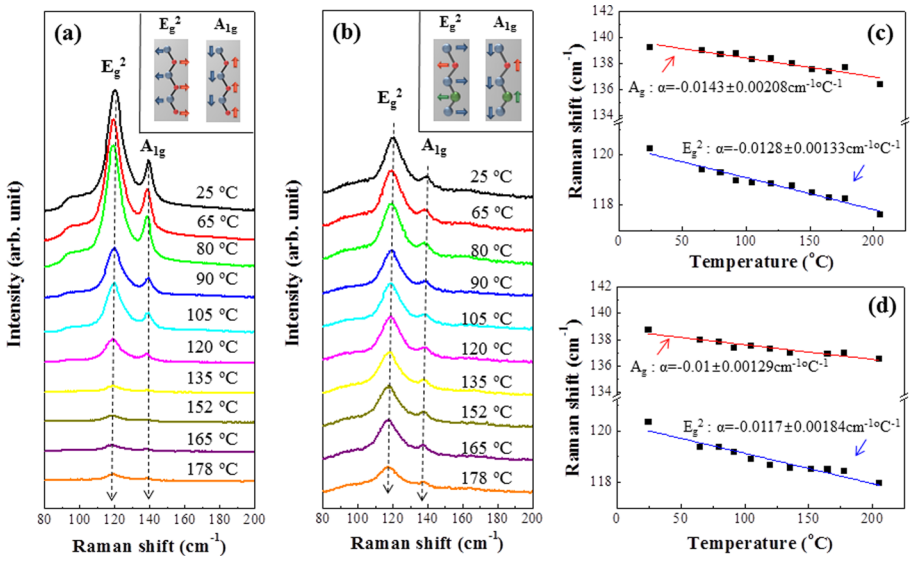

Figure 2. Raman spectra of (a) GeTe and (b) GST nanowire increasing temperature from 25 to 178 °C. (c) Plot of Raman peak shift versus temperature for the GeTe nanowire. Linear regression analysis yields a slope for of (a = −0.0128 ± 0.00133 cm^{-1} °C^{-1}) for E_g^2 and a = −0.0143 ± 0.00208 cm^{-1} °C^{-1} for A_{1g}. (d) plot of Raman peak shift versus temperature for the GST nanowire. The relation between Raman peak shift and temperature increase is linear with the value of (a = −0.0117 ± 0.00184 cm^{-1} °C^{-1} for E_g^2 and a = −0.01 ± 0.00129 cm^{-1} °C^{-1} for A_{1g}.

in a suspended nanowire. To confirm the feasibility of the method and to investigate the electrical operation characteristics of the GeTe and GST nanowires, the device was examined. The GeTe and GST nanowires were transferred to 50 nm SiO_2-deposited Si substrates with 12 electrodes of Ti/Au. After PMMA coating as an e-beam sensitive resistor(ER), an e-beam exposure was carried out with a Raith 50 e-beam writer in SEM. The ER was developed in an aqueous solution at room temperature. After development, a 20 nm thick Ti layer was deposited using a sputtering method and a lift-off process was then performed for contacts between the nanowire and Ti/Au metal pad.

RESULTS AND DISCUSSION

Figure 1a shows SEM images of as-grown GeTe nanowires. The diameters of the nanowires range from 80 to 160 nm with lengths of over 10 μm. The chemical composition of individual nanowires was also confirmed by EDS in scanning transmission electron microscopy (STEM), as shown in Figure 1b. The elemental mapping image of the nanowire clearly shows that elemental Ge and Te are uniformly distributed in the nanowire. Quantitative analysis by EDS point scanning confirms that Ge and Te are present in an atomic ratio of 1:1. HRTEM image selected area electron diffraction (SAED) patterns obtained from the GeTe nanowire in Figure 1c confirms that single-crystalline GeTe nanowire largely grow along the [110] direction. Moreover, clear lattice fringes with a spacing of 0.34 nm correspond to the distance between the (200) lattice planes on rhombohedral GeTe. The rhombohedral structure of the GeTe nanowire is consistent with a previous report of GeTe nanowires.[7] The SEM image of as-grown GST nanowires is presented in Figure 1d. The length and diameter of the nanowires are over 10 μm and typically 120−220 nm, respectively. The elemental mapping image of the GST nanowire shows that elemental Ge, Sb, and Te are uniformly distributed over the entire nanowire. The Ge/Sb/Te composition of the nanowire is 2:2:5. The indexed reciprocal lattices from HRTEM images and SAED patterns of GST nanowires show that the GST nanowire grows along the [110] direction, as shown in Figure 1f. The measured distance between two adjacent lattice planes, 0.212 nm, exactly corresponds to the (110) lattice plane of the GST hcp structure with a lattice constant a = 0.424 nm.[9]

Figure 2a shows the change in Raman spectra of GeTe nanowires with a temperature from 25 to 178 °C. As seen in the figure, two prominent peaks at ∼120 and ∼139 cm^{-1} corresponding to the E_g^2 mode and the A_{1g} mode, respectively, are present. Both the E_g^2 and A_{1g} modes are caused by a 2-fold degenerate state: in E_g^2, the atoms vibrate in the basal plane, while in A_{1g}, the atoms oscillate along the c-axis. The E_g^2 and A_{1g}, where the Ge and Te atoms move in opposite phase, are mainly affected by the forces between Ge and Te atoms (insert in Figure 2a). As the temperature increases, both Raman modes clearly soften linearly and broaden. Phonon anharmonicity is reflected through the temperature dependence of the Raman peak position and full width at half-maximum (fwhm). Since the variability in peak intensity (or fwhm) is sensitively dependent on beam focus and the position of the laser spot in a nanowire, the change in Raman peak position can provide more reliable information than the peak intensity. For this reason, only the temperature dependence of the peak position is considered. The Raman frequency depending on the temperature modulation is given by

$$\omega(T) = \omega_0 + \Delta_T(T) + \Delta_P(T) \quad (3)$$

where ω_0 is the harmonic frequency of the Raman mode, $\Delta_T(T)$ is the Raman frequency shift by thermal expansion, $\Delta_P(T)$ is the Raman frequency shift by anharmonic phonon−phonon coupling.[28] The shift in phonon energy by the movement of atomic position and variance in interatomic energy is caused by the lattice thermal expansion with increasing temperature.[25] Because the lattice thermal expansion has an effect on anharmonic vibrations of the lattice, the relationship between the Raman peak shift and temperature change is typically linear over room temperature.[12,25] Therefore, the equation for the temperature dependence on Raman peak shift expressed by $\Delta\omega = \alpha\Delta T$, where α, the slope of temperature (T) dependence, is the first-order temperature coefficient for the Raman mode. Figure 2c shows a plot of the

DOI: 10.1021/acsami.5b05703
ACS Appl. Mater. Interfaces 2015, 7, 21819−21827

Raman peak shift of E_g^2 and A_{1g} modes versus temperatures for the GeTe nanowire. From the frequency shift of Raman, a linear regression analysis yields a slope of $\alpha = -0.0128 \pm 0.00133$ cm^{-1} $°C^{1-}$ for E_g^2 and $\alpha = -0.0143 \pm 0.00208$ cm^{-1} $°C^{1-}$ for A_{1g}. $\alpha = -0.0143 \pm 0.00208$ cm^{-1} $°C^{1-}$ for A_{1g}. In the case of the GST nanowire, the Raman spectra with a temperature change from 25 to 178 °C and a plot of the Raman peak shift for the E_g^2 and A_{1g} modes versus temperature are shown in Figure 2b,d, respectively. In the Raman spectra, a change in the E_g^2 mode at ~119 cm^{-1} and the A_{1g} mode at ~138.7 cm^{-1} can be clearly observed, which is caused by the vibration of Ge (Sb) and Te atoms in opposite directions with respect to one another. Thus, A_{1g} and E_g^2 are mainly affected by both interatomic forces between the Ge and Te atoms and between Sb and Te atoms, respectively (insert in Figure 2a). The GST nanowire also shows a shift in Raman frequency with increasing temperature. The relationship for the Raman peak shift with temperature increase is linear with the value of $\alpha = -0.0117 \pm 0.00184$ cm^{-1} $°C^{1-}$ for E_g^2 and $\alpha = -0.01 \pm 0.00129$ cm^{-1} $°C^{1-}$ for A_{1g}.

To confirm the laser heating profile of the GeTe and GST nanowires, each nanowire was mechanically transferred to a Si substrate with Au line arrays with widths of 10 μm and heights of 150 nm. A schematic diagram and SEM image of the sample structure is shown in Figure 3. For the measurements,

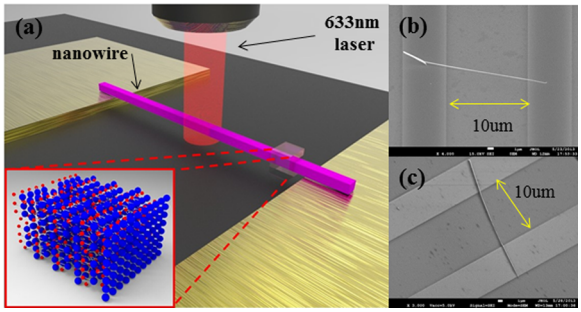

Figure 3. (a) Schematic diagram of sample structure. SEM image of mechanically transferred (b) GeTe nanowire and (c) GST nanowire on Au line array with 10 μm width and 150 nm height.

nanowires with a perpendicular length of 10 μm were freely suspended between the two Au lines. Raman scanning was performed from the edge of the nanowire to the opposite edge of the nanowire. The measurement of Raman frequency and heating by the Raman laser occurred at the same time when one laser source of 633 nm was used. Figure 4a shows the E_g^2 and A_{1g} Raman mode measured at 16 points along the length of a suspended GeTe nanowire. Since there is thermal heat sink when the nanowire is suspended from elemental Au, a downshift in the Raman spectra of about ~3.6 cm^{-1} is observed in the center of the suspended GeTe nanowire, compared to the value for the ends. From the results for Raman peak shift versus temperature change in the GeTe nanowire, we confirmed that the ΔT_{max} of E_g^2 and the A_{1g} Raman mode is 249.1 and 249.23 °C, respectively. Because the shift in the two peaks shows the similar tendency, the calculated ΔT_{max} is also nearly the same. In the case of the GST nanowire, as shown in Figure 4b, the maximum downshift of E_g^2 and A_{1g} Raman mode is ~2.1 cm^{-1} at the center of the GST nanowire. Using the relation of $\alpha = -0.01 \pm 0.00129$ cm^{-1} $°C^{1-}$ for A_{1g} and $\alpha = -0.0117 \pm 0.00184$ cm^{-1} $°C^{1-}$ for E_g^2, the estimated values of ΔT_{max}, 212.1 and 211.87 °C, can be obtained. For the evaluation of P_{abs} using FDTD, the optical constant n (refractive index) and k (extinction coefficient) of the GeTe and GST nanowires at 633 nm were obtained by DFT calculation. Figure 4c,d show the 2-D FDTD simulation results for GeTe and GST, respectively, i.e., the estimated value of the laser power absorbed by the GeTe and GST nanowires is 1.79×10^{-4}W and 1.53×10^{-4}W, respectively. In order to accurately calculate the value of absorbed laser power, with the structural information using SEM/TEM data, a nanowire with an appropriate shape was designed for the FDTD simulation. Next, the area of the nanowire was fixed as the absorbed region of laser. Because GeTe and GST have a thin native oxide layer (~5 nm thickness), the laser power absorbed by the nanowire was calculated with native oxide/nanowire structure. Using the value of ΔT_{max} and the laser power absorbed in the nanowire, the thermal conductivity of the GeTe and GST nanowires, 1.44 W/mK and 1.13W/mK, respectively, can be successfully evaluated. These values are smaller than previously reported values for thermal conductivity, obtained using polycrystalline thin films.[26,27] In addition, these thermal conductivity values are nearly the same as those obtained from electrical measurements (Figure S3).

Generally, as the dimension decreases, the surface to volume ratio increases.[28] Since this increase in the surface to volume ratio causes more scattering on the surface, the number of phonon collisions at the surface of nanowires exceeds that for a bulk material. As a result, the increase in phonon scattering multiplies the heat flow resistance, resulting in a reduction in the thermal conductivity. The surface to volume ratios of the GeTe and GST nanowires were measured by means of SEM and TEM. The average value of surface area to volume ratio of the GeTe and GST nanowires was determined to be 2.5×10^7/nm and 2.0×10^7/nm, respectively. These values are ~10 times higher than the reported values for a film. Therefore, the increase in the surface to volume ratio is the main factor for the reduction in thermal conductivity. Since as-grown nanowires of GeTe and GST have very smooth surfaces, the effect on thermal conduction caused by surface morphology cannot be a main factor for the low thermal conductivity of the as-grown nanowires. In addition, the native oxide (~5 nm) on the nanowire surface needs to be taken into consideration in the FDTD simulation. Surface band bending (SBB) caused by the native oxide was confirmed, as shown in Figure S4. The reported values for the energy differences between the Te $3d_{5/2}$ core-level and the valence band maximum (VBM) in both of the GeTe and GST films was found to be 573 eV. Compared with this value, the measured energy for SBB of 0.48 and 0.4 eV each in GeTe and GST nanowires is reasonable (Figure S4). The SBB in the GeTe and GST nanowire induces electron confinement at the surface. These localized surface charges owing to the nanostructure and SBB can critically enhance surface scattering, resulting in a significant decrease in thermal conductivity.

GeTe and GST based phase change memories use the resistance difference between two different phases, i.e., the amorphous and crystalline state through the set/reset processes by Joule heating. Therefore, the thermal property, especially the thermal conductivity value of GeTe and GST plays an important role in determining the evolution of the structural state during the rapid heating or cooling involved in memory operations. Since the GeTe and GST nanowires in this experiment have low thermal conductivity values, the phase transition process between the set/reset sates of GeTe and

DOI: 10.1021/acsami.5b05703
ACS Appl. Mater. Interfaces 2015, 7, 21819−21827

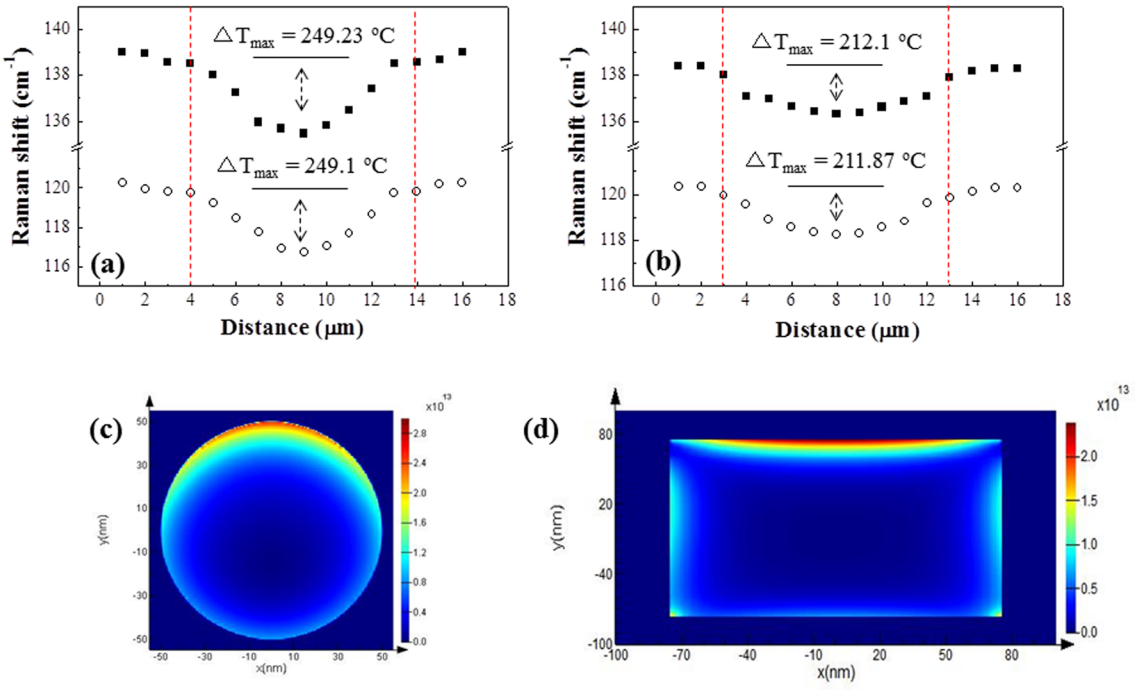

Figure 4. E_g^2 and A_{1g} Raman mode measured at 16 points along the length of a suspended (a) GeTe nanowire and (b) a GST nanowire. The ΔT_{max} of E_g^2 and A_{1g} Raman mode in the GeTe nanowire is 249.1 and 249.23 °C, respectively. In the GST nanowire, the ΔT_{max} of E_g^2 and A_{1g} Raman mode is 211.89 and 212.1 °C, respectively. 2-D FDTD simulation results of (c) GeTe and (d) GST, respectively. The estimated value of laser power absorbed in GeTe and GST nanowire is 1.79×10^{-4} W and 1.53×10^{-4} W, respectively.

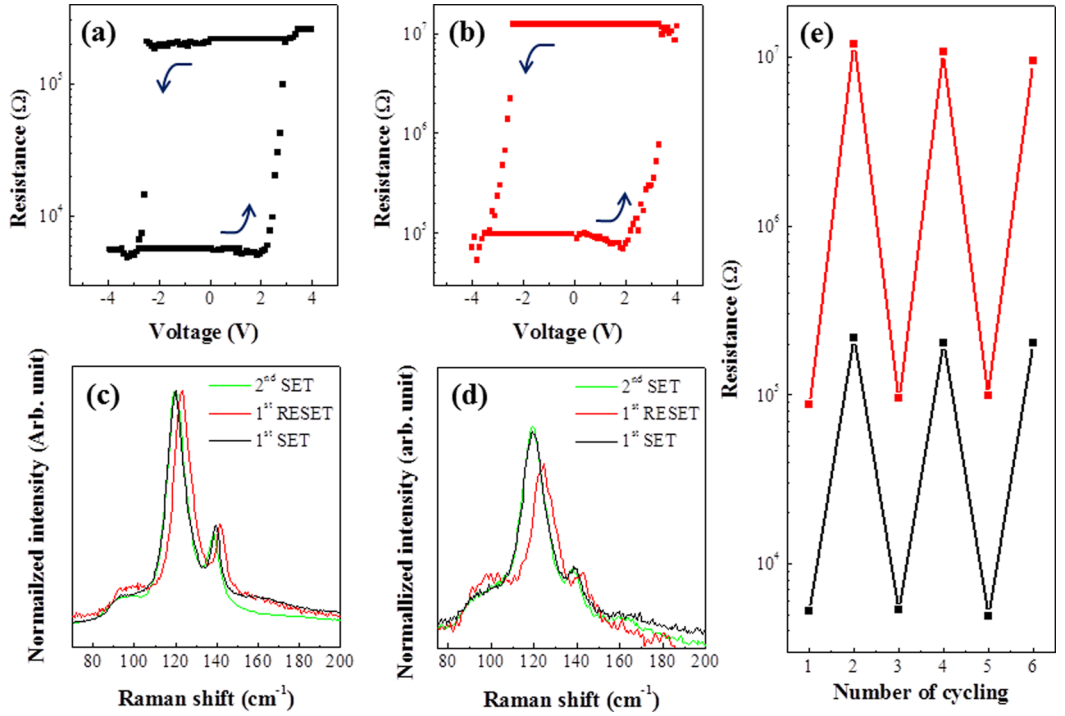

Figure 5. Bipolar memory switching property of (a) GeTe and (b) GST nanowire memory. Raman spectra of (c) GeTe and (d) GST nanowire according to the memory state. Because the size of the laser spot is ~1 μm and the value for the depth of field (DF) is ~3 μm at 633 nm, Raman analysis is suitable for confirming the change occurring in a local region of the nanowire. (e) Endurance characteristics of the GeTe (black square) and GST (red square) nanowire memory device with SET condition of 4 V/500 ns and RESET conditions of −4 V/500 ns.

GST nanowires can be affected by thermal conductivity. Figure 5a,b shows the memory switching properties of GeTe and GST nanowires, respectively. The initial resistances of GeTe and GST nanowire are ~5 kΩ and ~70 kΩ, respectively (Figure S5). Memory operation was investigated by increasing the applied voltage pulse time (20 ns to ~500 ns) and amplitude (0.0 V to ~4.0 V). Upon applying a voltage pulse at 500 ns and ~2.5 V, the resistance in the GeTe nanowire suddenly

DOI: 10.1021/acsami.5b05703
ACS Appl. Mater. Interfaces 2015, 7, 21819−21827

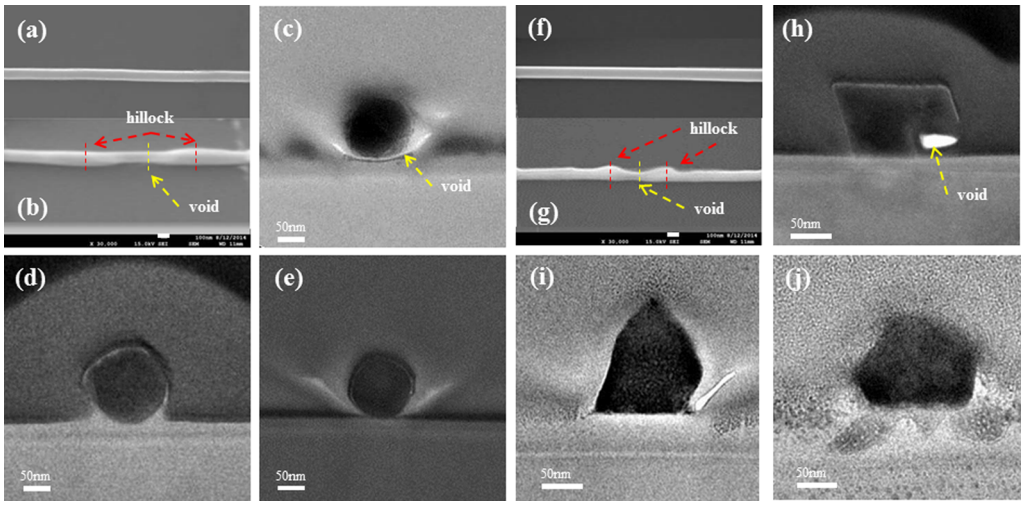

Figure 6. SEM image of (a) GeTe and (f) GST nanowire device before the memory operation. SEM image after the memory operation of (b) GeTe and (g) GST nanowires. After the memory operation, voids and hillocks are clearly seen in the nanowire. The cross-sectional TEM images of GeTe nanowire with a void (c) and hillocks (d,e) in device. The cross-sectional TEM images of GST nanowire with a void (h) and hillocks (i,j) in device.

increased and became saturated to ∼250 kΩ with a resistance ratio of over ∼50, compared to that of the initial state. In the case of the GST nanowire, the resistance was changed to ∼1.2 MΩ above ∼2.5 V with a resistance ratio of over ∼180, compared to that of the initial state. To return to the initial state of the crystalline GeTe and GST nanowire, an applied voltage pulse time was swept. Under a 500 ns voltage pulse, a change in resistance as a function of voltage change did not occur. Upon the applied voltage with a 500 ns pulse time from 4 V to −4 V, a drastic resistance drop in the GeTe and GST nanowire memory to initial value of the resistance occurred at ∼−2.5 V. Moreover, both of the nanowire devices show bipolar switching properties. The long reset time indicates that the sufficient Joule heating to permit phase change between amorphous and crystalline structure did not occur within this short operation time, under the low thermal conduction process. In order to confirm the durability of bipolar switching properties, an endurance test was performed. Figure 5e shows the endurance characteristics of a GeTe (black square) and a GST (red square) nanowire memory device with SET conditions of 4 V/500 ns and RESET condition of −4 V/500 ns. In previous reports, GeTe and GST nanowires have been reported to show unipolar operation through the phase change in the crystallization-amorphization state for SET/RESET.[29] Therefore, in order to confirm that the bipolar operation is unique and not unipolar, we investigated the initial, RESET, and SET states of the nanowires based on the change in Raman spectra, as shown in Figure 5c,d. Generally, characteristic Raman spectra clearly can show different features between the amorphous (RESET) and crystalline (SET) state, because the characteristic phonon vibration reflects the crystal structure and crystallinity of the material being measured. However, in both GeTe and GST nanowires, no change in the feature of the peaks was found. Only a Raman frequency shift between SET and RESET could be observed. In the case of the GeTe nanowire, in the first SET(initial) state, Raman peaks were observed at ∼120 and ∼139 cm^{-1}. After the RESET process, these peaks are shifted to ∼123 and 142 cm^{-1}. All peaks then return to the initial peak position by the second SET process. In the case of the GST nanowire, a very similar change in the peak shift was observed. That is, Raman peaks observed at ∼119 and ∼138.7 cm^{-1} in the initial state are shifted to ∼124.5 and ∼143.5 cm^{-1}, respectively, after the RESET process. After the second SET process, two peaks are then returned to the initial peak position. Such a change indicates that there is only structural modulation in the crystalline structure between the SET/RESET processes, without any structural transition between amorphous and crystalline structures. Therefore, the bipolar operation can be closely related with the structural modulation in maintaining the crystalline structure. Therefore, the change in resistance of the SET/RESET states is not caused by a structural phase transition between crystalline/amorphous structures. In order to confirm the structural modulation, we investigated the morphological shape between the SET/RESET processes. Interestingly, a morphological change was observed under the switching process. After the memory operation of GeTe and GST nanowires, the morphology of the nanowires were significantly changed from a smooth to a rough surface, as shown in Figure 6. In particular, voids and hillocks are clearly observed in the nanowires. This phenomenon is similar to the change caused by an electromigration of a nanowire.[30,31] Generally, pulsing the current in a nanowire, the generated thermal heat by the Joule process cannot uniform and the thermal conductivity is low. Under the thermal conduction process, the heat near the ends of the nanowires is easily transferred to the electrodes because the metal electrodes act as heat sinks at room temperature. On the other hand, the heat near the central part is not simply transferred to both electrodes because heat conduction is very low in the nanowires. Thus, since the heat accumulates in the central region of the nanowire during repeated pulsing, the temperature near the central region is dramatically increased.[32] As a result, the bonding strength between atoms at the central region becomes sufficiently weakened below the melting temperature. These weakened bonds are broken by electrical field stress, resulting in the generation of charged particles, which can be moved in a specific direction by the electrical field and wind force. Under this successive process, voids and hillocks as a result of the movement of charged atoms in local regions can be generated, thus causing a composition change in the local region of the nanowire. In addition, because the moved atoms are located in

DOI: 10.1021/acsami.5b05703
ACS Appl. Mater. Interfaces 2015, 7, 21819−21827

a crystal lattice, stress is generated. This stress causes a shift in the Raman frequency but not a change in fwhm.[33] The composition change in the void and hillock point of the GeTe and GST nanowire was investigated using TEM and EDS. Pt was deposited on the nanowire for preparing TEM samples and the devices were cut by FIB to include the nanowire with a small void and two hillocks. Figure 6c–e show the cross-sectional TEM images of the GeTe nanowire with a small void and two hillocks in a device. Regarding the void, the composition is similar to that of initial GeTe nanowire (EDS spectrum presented in Figure S7). On the other hand, the change in composition near the hillock is clearly observed. In the case of the hillock near the cathode, the amount of Ge is increased and the ratio of Ge:Te is changed to ~60:40 (see the EDS spectrum presented in Figure S7). In another hillock near the anode, the amount of Ge decreased and a ratio of Ge/Te became changed to 35:65 (see the EDS spectrum presented in Figure S7). In the case of the GST nanowire, the cross-sectional TEM image of the void and two hillock points are shown in Figure 6h,i,j, respectively. In the void point, the Ge/Sb/Te ratio is not changed conspicuously, compared with that of the initial GST nanowire (see the EDS spectrum presented in Figure S7). In the case of the two hillock points near the cathode and the anode, the tendency for the composition change in Ge and Te is similar to that for the GeTe nanowire. In addition, the change in the composition of Sb is similar to that for Ge near the cathode and anode. Thus, the GST composition is deficient in Ge and Sb in the hillock near the anode, while in the other hillock near the cathode, the GST composition is deficient in Te (see the EDS spectrum presented in Figure S7). The morphology and composition of the GeTe and GST nanowire are changed after the second SET. Although the morphology of the second SET is rougher than that of the initial state, voids and hillocks in nanowire are not clearly observed (details presented in Figure S8). However, the nonuniform contrast of the image caused by the difference in atomic content is observed as shown in Figure S8c, indicating that the morphology in a local region is not fully recovered to the initial state. Through the phenomena of void and hillock generation and composition change, the bipolar switching property can be explained by electromigration. In addition, on the basis of these phenomena, the resistance of the nanowire is changed. Because the area in which a current can flow is reduced by a void and the void itself hinders the electrical conduction process, the resistance of the nanowire is increased. Moreover, segregated atoms also increase electron scattering. In the electromigration of an alloy, the compositional change can be attributed to the ionicity of atoms. In the case of GeTe and GST, since the electronegativity value of Te is higher than Sb and Ge (4.6 eV for Ge, 4.85 eV for Sb, and 5.49 eV for Te), Te loses electrons easier than Ge and Sb.[34] In other words, Ge and Sb function as cations, while Te functions as an anion under high current pulse in GST. In addition, Ge functions as a cation, while Te functions as an anion under the pulse in GT. Therefore, in the case of the GeTe nanowire, Ge and Te atoms start moving from the middle region of the nanowire to the cathode and anode, respectively, because the temperature of the middle region far from the heat sink of the metal electrode is higher than that of the edge of the wire near the metal electrode. A schematic diagram of atomic moving of GeTe nanowire is presented in Figure 7a. In the GST nanowire, Ge and Sb atoms move toward the cathode and Te atoms move toward the anode. The schematic diagram of the movement of

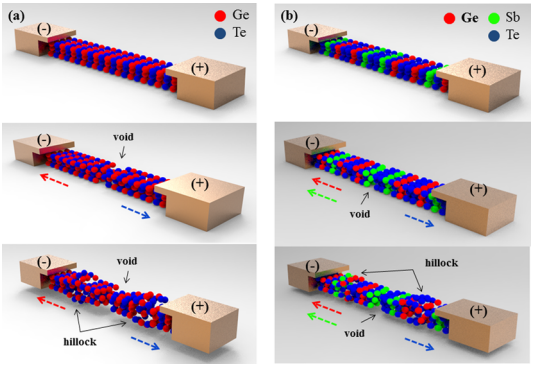

Figure 7. Schematic diagram of the process by which voids and hillocks are formed in (a) GeTe and (b) GST nanowires.

atoms in the GST nanowire is presented in Figure 7b. By electromigration, an analysis of Raman spectra, STEM, and EDS data confirms that an electromigration mainly affects the bipolar memory property in GeTe and GST nanowire memories. In the GeTe and GST nanowires with a low thermal conductivity, sufficient heat for a phase change from the crystalline to amorphous state is not generated to permit it to be transferred to the middle region of a long nanowire. Moreover, after the RESET process, the value of the thermal conductivity in the GeTe and GST nanowires still remained low, because the formation of voids, hillocks, and interfaces between voids and hillocks increases the scattering of carriers and hinders phonon transport. Consequently, sweeping the pulse into the GeTe and GST nanowire, electromigration occurs instead of phase change. Moreover, the current path can be affected by atomic motion during the electromigration process, which also contributes to bipolar memory operation. Generally, reversible unipolar electrical switching in a phase change device occurs between the amorphous and metastable states.[3,4,6] However, because of the low resistance and stable structure in the crystalline state of GeTe and GST, reversible electrical switching is very difficult.[3,4,6] In a previous report,[9] Nam et. al explained the mechanism of resistance change in hexagonal single crystalline GST nanowire using dislocation moving by electromigration. Because, in GST, the hexagonal structure is a stable state, phase change from a hexagonal structure to an amorphous phase using Joule heating would be very difficult. In this study, as can be seen in Figure 1, the grown nanowires show a stable crystalline structure. Therefore, bipolar memory switching by electromigration is more dominant than unipolar switching with a phase change in GeTe and GST nanowires. For these reasons, to design a memory device using chalcogenide materials, thermal conductivity and structural stability should be considered.

CONCLUSION

In conclusion, we report on the thermal conductivity of single-crystal GeTe and GST nanowires using Raman spectroscopy. The obtained thermal conductivity values for GeTe and GST nanowires at room temperature show significantly lowered values with 1.44 Wm^{-1} K^{-1} for GeTe and 1.13 Wm^{-1} K^{-1} for GST in comparison with previously reported values. These low thermal conductivity values are caused by a combination of an increase in the surface to volume ratio and surface band bending in the nanowire. We also investigated the memory characteristics of the single-crystalline GeTe and GST nanowires with very low thermal conductivity. The SET/RESET

DOI: 10.1021/acsami.5b05703
ACS Appl. Mater. Interfaces 2015, 7, 21819–21827

characteristics as a memory device using the GeTe and GST nanowires show that electromigration occurs by the low thermal conductivity value instead of the phase change because sufficient heat for the phase change cannot be transferred to the middle region of long GeTe and GST nanowires. In addition, because the GeTe and GST nanowire has stable crystal structure, a phase change using Joule heating is difficult. As a result, the memory operation involves bipolar properties. Since the electromigration under the electrical operation is closely related to the thermal conductivity, the effect of electromigration is enhanced in the device structure with its length. Therefore, the thermal conduction represents a very important problem concerning the reliability of a device. Fortunately, because the effect can be decreased by virtue of the scale-down of a device, the effect of low thermal conduction in a nanosized device is not likely to be critical. Nevertheless, the difference in thermal conduction at the interface of a device structure can potentially affect its reliability. However, the change in resistivity with structural variation under maintaining the crystalline structure suggests the possibility of a new device operation, provided that the electromigration effect can be delicately controlled.

■ ASSOCIATED CONTENT

Supporting Information

The Supporting Information is available free of charge on the ACS Publications website at DOI: 10.1021/acsami.5b05703.

Diameter distributions of nanowires; electron diffraction pattern of nanowires; thermal conductivity data of GST nanowire; XPS core-level spectra of nanowire; *I*−*V* characteristic of nanowire; bipolar memory switching property of nanowire; EDS spectrum of void and hillocks in nanowire; and cross-sectional SEM, TEM, and EDS data of nanowire after 2nd SET process (PDF)

■ AUTHOR INFORMATION

Corresponding Author

*E-mail: mh.cho@yonsei.ac.kr.

Present Address

⊥S.P.: Process Development Team, Samsung Semiconductor R & D Center, Hwasung 445-701, Korea.

Notes

The authors declare no competing financial interest.

■ ACKNOWLEDGMENTS

This work was supported by the National Research Foundation of Korea (NRF) grant funded by the Korea government (MSIP) (Grant No. 2015R1A2A1A01007560) and the MOTIE (Ministry of Trade, Industry & Energy (Project Number 10045360) and KSRC (Korea Semiconductor Research Consortium) support program for the development of the future semiconductor device. We thank KBSI Woong-Ki Hong at the Jeonju of the Korean Basic Science Institute for the technical assistance in Raman spectroscopy.

■ REFERENCES

(1) Zhou, X.; Xia, M.; Rao, F.; Wu, L.; Li, X.; Song, Z.; Feng, S.; Sun, H. Understanding Phase-Change Behaviors of Carbon-Doped $Ge_2Sb_2Te_5$ for Phase-Change Memory Application. *ACS Appl. Mater. Interfaces* **2014**, *6*, 14207−14214.

(2) Park, S. J.; Jang, M. H.; Park, S. J.; Ahn, M.; Park, D. B.; Ko, D.; Cho, M. H. Effect of amorphization on the structural stability and reversibility of $Ge_2Sb_2Te_5$ and oxygen incorporated $Ge_2Sb_2Te_5$ films. *J. Mater. Chem.* **2012**, *22*, 16527−16533.

(3) Park, W. I.; You, B. K.; Mun, B. H.; Seo, H. K.; Lee, J. Y.; Hosaka, S.; Yin, Y.; Ross, C. A.; Lee, K. J.; Jung, Y. S. Self-Assembled Incorporation of Modulated Block Copolymer Nanostructures in Phase-Change Memory for Switching Power Reduction. *ACS Nano* **2013**, *7*, 2651−2658.

(4) Piekiel, N. W.; Cavicchi, R. E.; Zachariah, M. R. Rapid-heating of energetic materials using a micro-differential scanning calorimeter. *Thermochim. Acta* **2011**, *521*, 125−129.

(5) Graydon, O. Non-volatile storage. *Nat. Photonics* **2013**, *7*, 2.

(6) Rosenthal, T.; Schneider, M. N.; Stiewe, C.; Döblinger, M.; Oeckler, O. Real Structure and Thermoelectric Properties of GeTe-Rich Germanium Antimony Tellurides. *Chem. Mater.* **2011**, *23*, 4349−4356.

(7) Yang, C. L.; Lai, H. J.; Hwang, J. D.; Chuang, T. H. Diffusion Soldering of Pb-Doped GeTe Thermoelectric Modules with Cu Electrodes Using a Thin-Film Sn Interlayer. *J. Electron. Mater.* **2013**, *42*, 359−365.

(8) Sa, B.; Zhou, J.; Sun, Z.; Ahuja, R. Strain-induced topological insulating behavior in ternary chalcogenide $Ge_2Sb_2Te_5$. *Europhys. Lett.* **2012**, *97*, 27003.

(9) Nam, S. W.; Chung, H. S.; Lo, Y. C.; Qi, L.; Li, J.; Lu, Y.; Johnson, A. T. C.; Jung, Y.; Nukala, P.; Agarwal, R. Electrical Wind Force−Driven and Dislocation-Templated Amorphization in Phase-Change Nanowires. *Science* **2012**, *336*, 1561−1566.

(10) Sun, X.; Yu, B.; Ng, G.; Meyyappan, M. One-Dimensional Phase-Change Nanostructure: Germanium Telluride Nanowire. *J. Phys. Chem. C* **2007**, *111*, 2421−2425.

(11) Nukala, P.; Agarwal, R.; Qian, X.; Jang, M. H.; Dhara, S.; Kumar, K.; Johnson, A. T. C.; Li, J.; Agarwal, R. Direct Observation of Metal−Insulator Transition in Single-Crystalline Germanium Telluride Nanowire Memory Devices Prior to Amorphization. *Nano Lett.* **2014**, *14*, 2201−2209.

(12) Burke, H. H.; Herman, I. P. Temperature dependence of Raman scattering in Ge1−xSix alloys. *Phys. Rev. B: Condens. Matter Mater. Phys.* **1993**, *48*, 15016−15024.

(13) Stranz, A.; Waag, A.; Peiner, E. Thermal characterization of vertical silicon nanowires. *J. Mater. Res.* **2011**, *26*, 1958−1962.

(14) Hu, Z. J.; Padilla, A. A.; Xu, J.; Fisher, T. S.; Goodson, K. E. 3-Omega Measurements of Vertically Oriented Carbon Nanotubes on Silicon. *J. Heat Transfer* **2006**, *128*, 1109−1113.

(15) Balandin, A.; Ghosh, S.; Bao, W.; Calizo, I.; Teweldebrhan, D.; Miao, F.; Lau, C. Superior Thermal Conductivity of Single-Layer Graphene. *Nano Lett.* **2008**, *8*, 902−907.

(16) Ghosh, S.; Bao, W.; Nika, D.; Subrina, S.; Pokatilov, E.; Lau, C.; Balandin, A. Dimensional crossover of thermal transport in few-layer graphene. *Nat. Mater.* **2010**, *9*, 555−558.

(17) Balandin, A. Thermal properties of graphene and nanostructured carbon materials. *Nat. Mater.* **2011**, *10*, 569−581.

(18) Renteria, J.; Ramirez, S.; Malekpour, H.; Alonso, B.; Centeno, A.; Zurutuza, A.; Cocemasov, A.; Nika, D.; Balandin, A. Strongly Anisotropic Thermal Conductivity of Free-Standing Reduced Graphene Oxide Films Annealed at High Temperature. *Adv. Funct. Mater.* **2015**, *25*, 4664−4672.

(19) Yan, Z.; Jiang, C.; Pope, T.; Tsang, C.; Stickney, J.; Goli, P.; Renteria, J.; Salguero, T.; Balandin, A. Phonon and thermal properties of exfoliated $TaSe_2$ thin films. *J. Appl. Phys.* **2013**, *114*, 204301.

(20) Soini, M.; Zardo, I.; Uccelli, E.; Funk, S.; Koblmüller, G.; Morral, A. F. I.; Abstreiter, G. Thermal conductivity of GaAs nanowires studied by micro-Raman spectroscopy combined with laser heating. *Appl. Phys. Lett.* **2010**, *97*, 263107.

(21) Doerk, G. S.; Carraro, C.; Maboudian, R. Temperature Dependence of Raman Scattering in Silicon. *Phys. Rev. B: Condens. Matter Mater. Phys.* **2009**, *1*, 638−642.

(22) Doerk, G. S.; Carraro, C.; Maboudian, R. Single Nanowire Thermal Conductivity Measurements by Raman Thermography. *ACS Nano* **2010**, *4*, 4908−4914.

DOI: 10.1021/acsami.5b05703
ACS Appl. Mater. Interfaces 2015, 7, 21819−21827

(23) Malekpour, H.; Chang, K.-H.; Chen, J.-C.; Lu, C.-Y.; Nika, D. L.; Novoselov, K. S.; Balandin, A. A. Thermal Conductivity of Graphene Laminate. *Nano Lett.* **2014**, *14*, 5155−5161.
(24) Oskooi, A. F.; Roundy, D.; Ibanescu, M.; Bermel, P.; Joannopoulos, J. D.; Johnson, S. G. Meep: A flexible free-software package for electromagnetic simulations by the FDTD method. *Comput. Phys. Commun.* **2010**, *181*, 687−702.
(25) Beechem, T.; Graham, S.; Kearney, S. P.; Phinney, L. M.; Serrano, J. R. Invited Article: Simultaneous mapping of temperature and stress in microdevices using micro-Raman spectroscopy. *Rev. Sci. Instrum.* **2007**, *78*, 061301.
(26) Lyeo, H. K.; Cahill, D. G.; Lee, B. S.; Abelson, J. R.; Kwon, M. H.; Kim, K. B.; Bishop, S. G.; Cheong, B. K. Thermal conductivity of phase-change material $Ge_2Sb_2Te_5$. *Appl. Phys. Lett.* **2006**, *89*, 151904.
(27) Fallica, R.; Varesi, E.; Fumagalli, L.; Spadoni, S.; Longo, M.; Wiemer, C. Effect of nitrogen doping on the thermal conductivity of GeTe thin films. *Phys. Status Solidi RRL* **2013**, *7*, 1107−1111.
(28) Pan, H.; Feng, Y. P. Semiconductor Nanowires and Nanotubes: Effects of Size and Surface-to-Volume Ratio. *ACS Nano* **2008**, *2*, 2410−2414.
(29) Park, S. J.; Kim, I.; Kim, S.; Yoon, S.; Yu, B.; Choi, S. Phase transition characteristics and device performance of Si-doped $Ge_2Sb_2Te_5$. *Semicond. Sci. Technol.* **2008**, *23*, 105006.
(30) Song, T. B.; Chen, Y.; Chung, C. H.; Yang, Y.; Bob, B.; Duan, H. S.; Li, G.; Tu, K. N.; Huang, Y.; Yang, Y. Nanoscale Joule Heating and Electromigration Enhanced Ripening of Silver Nanowire Contacts. *ACS Nano* **2014**, *8*, 2804−2811.
(31) Esen, G.; Fuhrer, M. S. Temperature control of electromigration to form gold nanogap junctions. *Appl. Phys. Lett.* **2005**, *87*, 263101.
(32) Yasunaga, H.; Natori, A. Electromigration on semiconductor surfaces. *Surf. Sci. Rep.* **1992**, *15*, 205−280.
(33) Murphy, K.; Piccione, B.; Zanjani, M.; Lukes, J.; Gianola, D. S. Strain- and Defect-Mediated Thermal Conductivity in Silicon Nanowires. *Nano Lett.* **2014**, *14*, 3785−3792.
(34) Pearson, R. Absolute electronegativity and hardness: application to inorganic chemistry. *Inorg. Chem.* **1988**, *27*, 734−740.

DOI: 10.1021/acsami.5b05703
ACS Appl. Mater. Interfaces 2015, 7, 21819−21827